

THE EFFECT OF THE EXTENT OF CORAL REEF AREA ON UNIFORM BOTTOM REFLECTANCE DETERMINATION FOR WATER COLUMN CORRECTION USING LANDSAT ETM

Syarif Budhiman^{1*}, Ety Parwati¹, and Emiyati¹

¹Remote Sensing Application Center, National Institute of Aeronautics and Space (LAPAN)

*E-mail: syarif.budhiman@lapan.go.id

Abstract. In one pixel of 30 meter spatial resolution of Landsat ETM multispectral sensor might consist of mixed bottom substrate types. The influence of a mixture of bottom substrate on the Landsat data can be a source of errors and together with the extent of coral reef area might contribute to affect the determination of uniform bottom reflectance. This study aimed to assess the effect of the extent of coral reef area on uniform bottom reflectance determination for water column correction. Lyzenga method was used for water column correction. This study carried out in two case studies using two sites with different size of coral reef ecosystems area i.e., Tidung island, in the Province of Jakarta and Maratua island, in the Province of East Kalimantan. Tidung island was selected to represent small area of coral reef ecosystem, while Maratua island was selected to represent relatively larger area of coral reef ecosystem. The results showed that the extent of coral reef influenced the determination of training sample areas for uniform bottom reflectance using Landsat ETM. The combination of moderate spatial resolution and the small area of coral reef ecosystem lead to the difficulties for uniform bottom substrate type determination at different depths.

Keywords: coral reef, Landsat ETM, water column correction

1 INTRODUCTION

Many researches on the utilization of remote sensing data for the identification and mapping of coral reefs have been carried out (Maritorea, 1996, Rauf and Yusuf, 2004, Vanderstraete *et al.*, 2004, Suciati and Arthana, 2008, Eakin *et al.*, 2010, Siregar, 2010, Hamylton, 2011, Helmi *et al.*, 2011, Contreras-Silva *et al.*, 2012, Hedley *et al.*, 2012a). Landsat 7 data with Enhanced Thematic Mapper (ETM) sensor was used in many studies (Andrefouet *et al.* 2001, Adi, 2003, Joyce *et al.*, 2004). Moreover, NASA (National Aeronautics and Space Administration) conducted a global mapping of coral reefs using Landsat 7 ETM (<http://oceancolor.gsfc.nasa.gov/cgi/landsat.p1>). A number of 1490 scenes of Landsat 7 ETM data with acquisition date from 1999 to 2003 were analyzed for that purpose.

In this study we used the Lyzenga technique for water column correction. This method proposed to discriminate various bottom types using multispectral image data sets with an initial assumption that the radiance ratios of two distinct bottom substrate would be independent of water

depth as long as the attenuation coefficients are the same. The main problem is how to distinguish various bottom substrates and to find uniform bottom reflectance within the 30 meter spatial resolution of Landsat ETM. Yamano and Tamura (2004) described the limitation of spatial resolution of Landsat TM (Thematic Mapper) in mapping coral reef bleaching (the spatial resolution of Landsat TM is similar to spatial resolution of Landsat ETM). The sensor limitation in 30 meter spatial resolution could lead to unclear bottom substrate identification. Hedley *et al.* (2012b) explained that based on heterogeneity in coral reefs environment, it would require spatial resolution less than 1 m. The discrepancy in spatial resolution between Landsat ETM and the scale of homogeneity of substrate distribution could lead to the existence of mixed pixel (Purkis and Pasterkamp, 2004), therefore the size of the coral reef ecosystem area could contribute to the problem. Consequently, the problem in identifying uniform bottom substrate could influence the calculation of the water column correction.

Based on these problems, the purpose of this study was to assess the effect of the extent of coral reef area on uniform bottom reflectance determination for water column correction. This study was carried out in two different sites with different size of coral reef ecosystems i.e., Tidung island, in the Province of Jakarta and Maratua island, in the Province of East Kalimantan.

2 MATERIALS AND METHOD

2.1 Study area

Tidung island and Maratua island were selected to represent small area and relatively larger area of the coral reef ecosystem (Figure 1). Tidung island at Kepulauan Seribu regency consists of two islands i.e., Pulau Tidung Besar on the west side and Pulau Tidung Kecil on the east side, with an area of 50 ha and 17 ha, respectively. The whole area of Tidung island, including the coral reef ecosystem, covers approximately 109 ha (www.pulau-tidung.com). On the contrary, the land of Maratua island covers

an area of 2282 ha. Maratua island in East Kalimantan is an atoll with open lagoon water connected with surrounding sea water. The whole area of Maratua island, including the coral reef ecosystem, covers approximately 69000 ha (Wiryawan *et al.*, 2005). The different area between Tidung island and Maratua island are expected to demonstrate the effect of the extent of coral reef area on uniform bottom reflectance determination for water column correction using Landsat ETM data.

2.2 Data

This study used Landsat ETM and WordView-2 data. Two Landsat ETM data of Tidung island acquired on September 17, 2001 and Landsat ETM data of Maratua island, acquired on July 8, 2002 were used. Landsat data has 30 m spatial resolution and consists of 8 bands, and only three bands can penetrate to water column with the wavelength range between 450 nm to 690 nm (NASA, 2012). The Landsat satellite

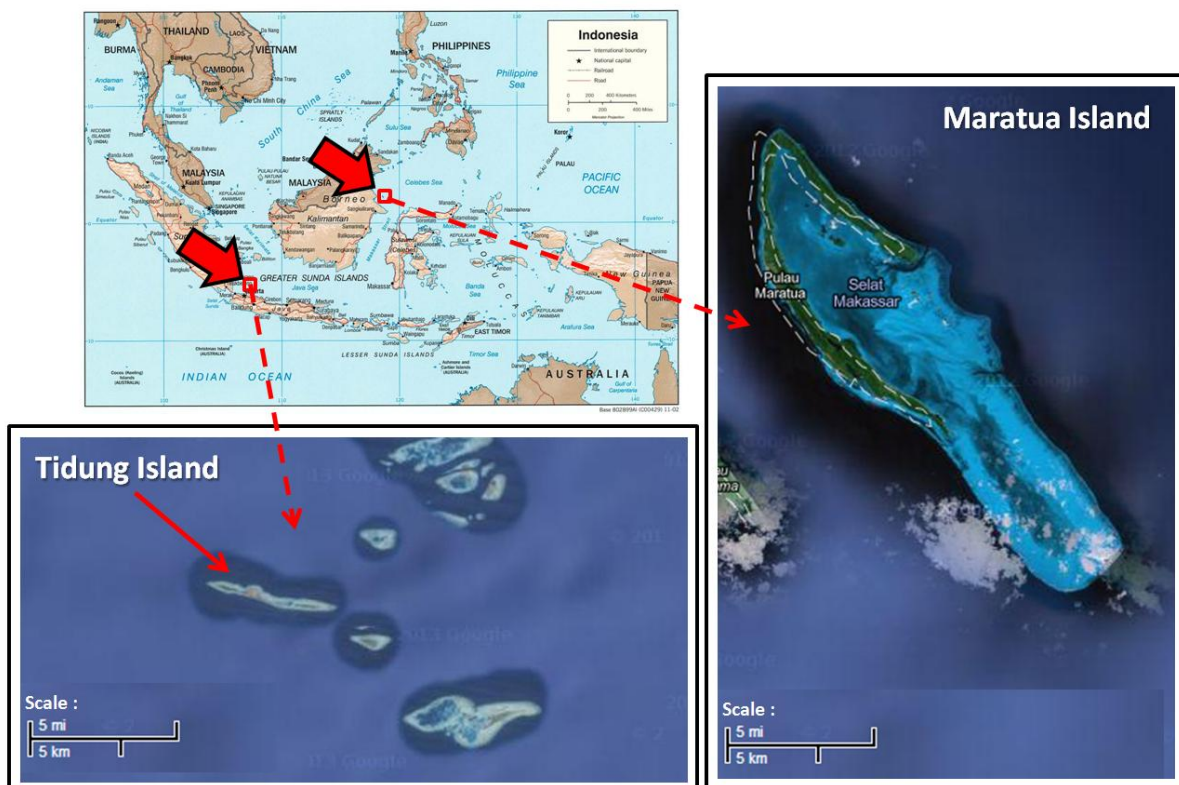


Figure 1. The location of Tidung island and Maratua island.

data acquired before slc-off (before 2003) were selected to minimize the error by the missing part from the data due to technical problem during data acquisition. Moreover, the selection of data before slc-off had been proposed by The Millennium Coral Reef Mapping Project, NASA (<http://oceanscolor.gsfc.nasa.gov/LANDSAT/HTML/README.html>).

WorldView-2 data of Tidung island acquired on December 4, 2011 was used to compare the capability of different spatial resolution to distinguish bottom substrate. WorldView-2 has 50 cm spatial resolution in panchromatic and 1,84 m in multispectral bands and consists of 8 bands. The data was received from LAPAN.

2.3 Digital number (DN) to radiance conversion

Digital number of Landsat data were converted to radiance value by equation (NASA, 2012):

$$L_i = \left(\frac{LMax_i - LMin_i}{QCalMax - QCalMin} \right) * (QCal - QCalMin) + LMin_i \quad (1)$$

where L_i is radiance value on band i , $LMax_i$ is radiance value maximum on band i , $LMin_i$ is radiance value minimum on band i , $QCalMax$ is maximum pixel value in Digital

Number (DN=255), $QCalMin$ is minimum pixel value in Digital Number (DN=1), and $Qcal$ is pixel in Digital Number which to be converted to radiance.

2.4 Atmospheric correction

Rough atmospheric correction was done using dark pixel subtraction method based on radiance value on optically deep sea water area for each Landsat ETM bands. Visible light mostly absorbed within the optically deep water and the remaining value were account for atmospheric radiance. Armstrong (1993) suggested to subtract the mean deep water radiance with its standard deviation for possible sensor noise (UNESCO, 1999; Green *et al.*, 2000). The remaining radiance

subtract radiance value for value was used to each pixel in Landsat ETM bands.

2.5 Water column correction

Water column correction was done in accordance with Lyzenga method (1981). The radiance measurements were performed on the same type bottom substrate with different depth, subsequently the radiance value of band i dan j will correlated linearly. The slope in the linear correlation equation was the approximation of attenuation coefficient ratio between band i dan j . The equation is written as (Green *et al.*, 2000):

$$\text{depth invariant index} = \ln(L_{atcor_i}) - \frac{k_i}{k_j} (\ln(L_{atcor_j})) \quad (2)$$

where L_{atcor} is radiance after atmospheric correction for band i dan j , and k_i/k_j is coefficient of attenuation. The k_i/k_j was calculated from the root mean square of minimum deviation to the linear correlation line (Lyzenga, 1981).

$$\frac{k_i}{k_j} = a + \sqrt{a^2 + 1} \quad (3)$$

$$a = \frac{\sigma_{ii} - \sigma_{jj}}{2\sigma_{ij}} \quad (4)$$

where σ_{ii} is variance value of band i , σ_{jj} is variance value of band j , dan σ_{ij} is covariance value of band i and band j .

2.6 Evaluation

Several authors (Armstrong, 1993; Geen *et al.*, 2000; Vanderstraete *et al.*, 2004) have published their ratios of attenuation coefficient using the 30 meter Landsat spatial resolution. The mentioned literature results were used as standard of the ratio

attenuation coefficient. Evaluation of the result was conducted by comparing the results of ratio attenuation from Tidung island and Maratua island case study with the results from literatures. Although the ratio could vary according to the specific water types being

sampled, however in this study an assumption of the same water types (clear water) was used. The whole research flowchart is shown in Figure 2.

3 RESULTS AND DISCUSSION

3.1 Case study of Tidung island, Kepulauan Seribu, Jakarta

WorldView-2 data and Landsat ETM data were compared visually in order to observe their ability to identify object and the proportion of mixed pixel. Shallow water bottom substrate was clearly visible in WorldView-2 (Figure 3a), whereas it was not visible in Landsat (Figure 3b). The high proportion of mixed pixel in Landsat data was clearly shown in figure 3 (some pixel showed mixed information of sand and seagrass). It was hard to find a homogeneous bottom substrate at different depth due to relatively small area of the island that covered by Landsat spatial resolution. The training sample was conducted within the bright pixel in shallow water part of Tidung

island, assumed that the depth were slightly different (Figure 4).

Equation 2-4 was applied for three pairs of Landsat spectral bands that can penetrate through water column (band 1, band 2, and band 3). Lyzenga (1981) has suggested using multi depth-invariant index approach in order to extract bottom substrate information. 10 training samples site were selected (Figure 4) with total of 124 pixels. Figure 5 shows the graph between two Landsat bands in logarithmic scale and its attenuation coefficient (k_i/k_j). The result of the ratio k_i/k_j are 1.2094, 1.2211 and 0.9939 respectively. The graphs in Figure 5 were based on sand type bottom substrate.

Figure 6b shows the results of Lyzenga method. The result shows a small range of depth-invariance index value. The bottom substrate in Figure 6b (in purple color) represent the same bottom substrate with bright white color in Figure 6a. This bottom substrate can be identified as mixed

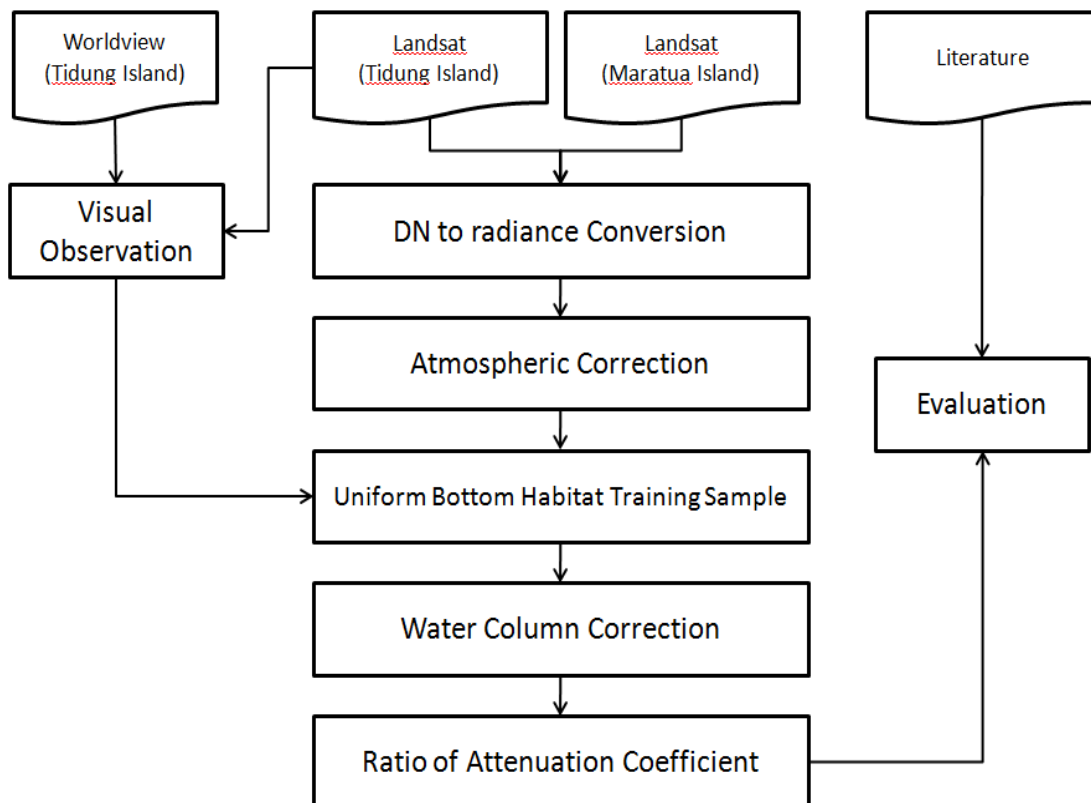


Figure 2. The research flowchart

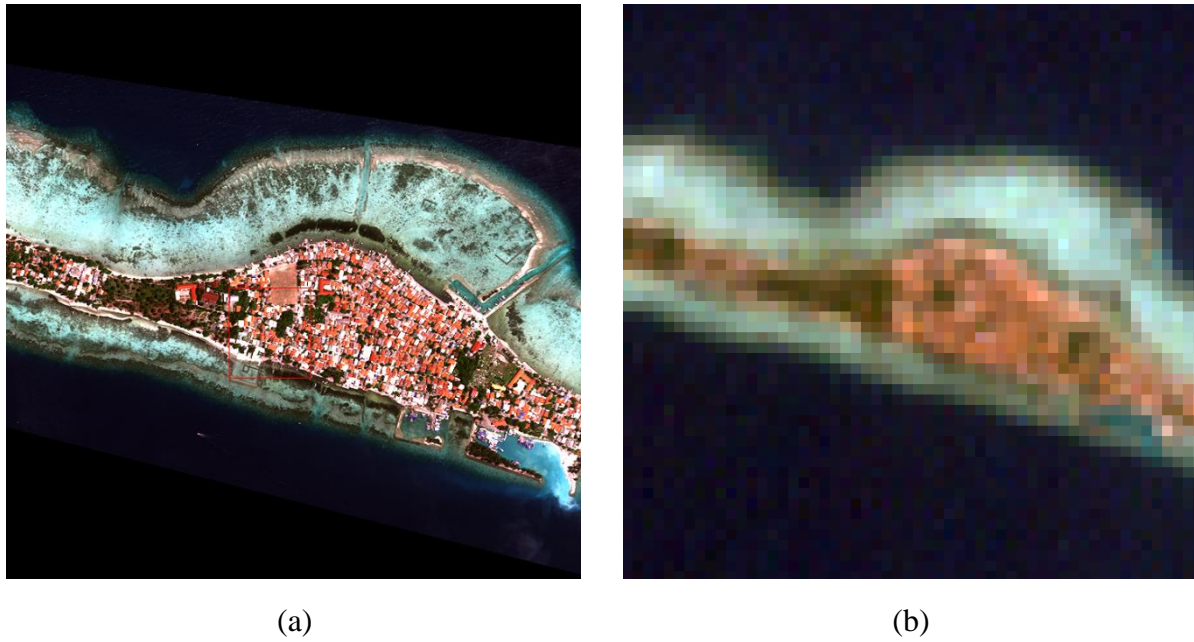


Figure 3. Image of Tidung island from WorldView-2 (a) and Landsat ETM (b).

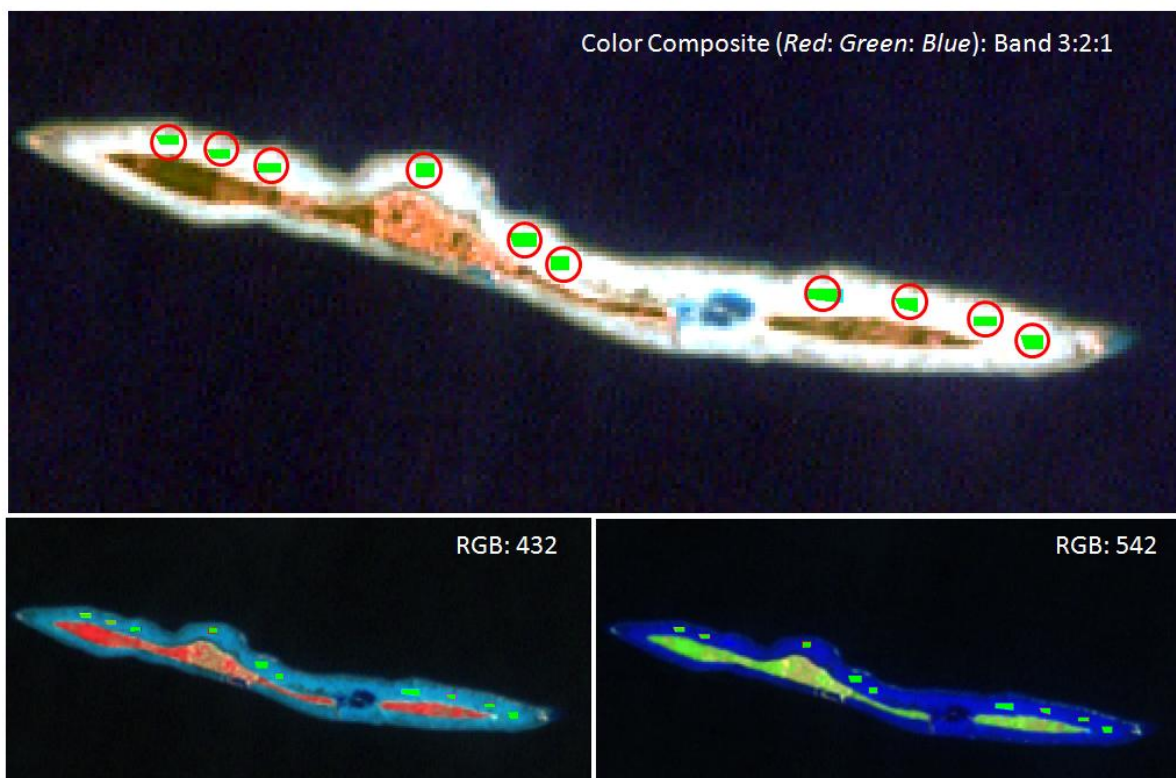


Figure 4. Three different color composite of Landsat ETM (RGB 321, RGB 432 dan RGB 542) of Tidung island and training sample site selection (circled).

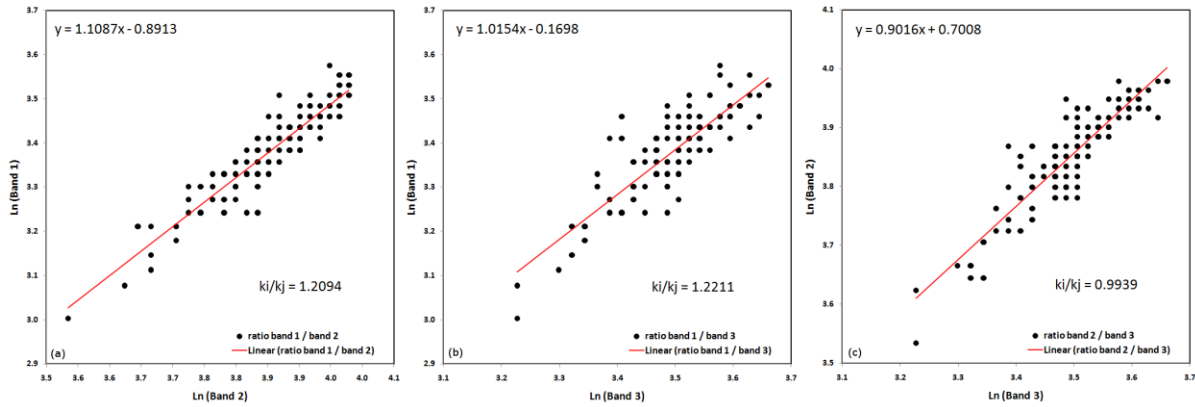


Figure 5. Graph of two pair bands in logarithmic scale and its coefficient attenuation ratio for Tidung island image using ratio of band 1 and band 2 (a), ratio of band 1 and band 3 (b), and ratio of band 2 and band 3 (c).

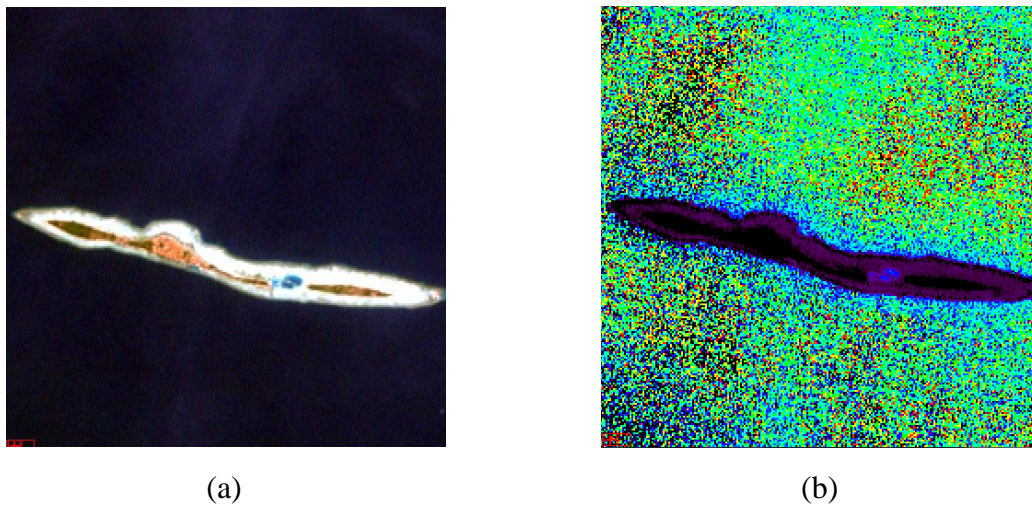


Figure 6. True color composite RGB 321 (a) and Lyzenga (b).

bottom substrate of sand and seagrass (Figure 3a). However, due to limitation of Landsat spatial resolution, one cannot distinguish two different bottom substrates within one pixel. Figure 7b shows the value of band 1, band 2, band 3 and depth-invariant index calculated from Lyzenga method. Pixel positions are in x-axis, where pixel number 1-8 shows the area within the island, and pixel number 9-16 are the deep water. The graph shows that the result from Lyzenga (Equation 2) shows different trend (circled line). with the transect line between pixel 1 until pixel 8 has relatively the same index value, which is indicated the same bottom substrate type (sand dominated type).

3.2 Case study of Maratua island, East Kalimantan

In this case study, the training sample sites were selected in area presumably as sand. Sand gives brighter color than the surrounding, because most of the incoming light will be reflected back. This characteristic was used as reference for training sample site selection. Figure 8 shows all the training sample sites. The differences of color composite were useful to help distinguish the difference in depth (Figure 8). The brighter the object color indicated that the water depth become shallower. The differences composite also help to distinguish open water sand and underwater sand, whereas the training sample only selected the underwater sand.

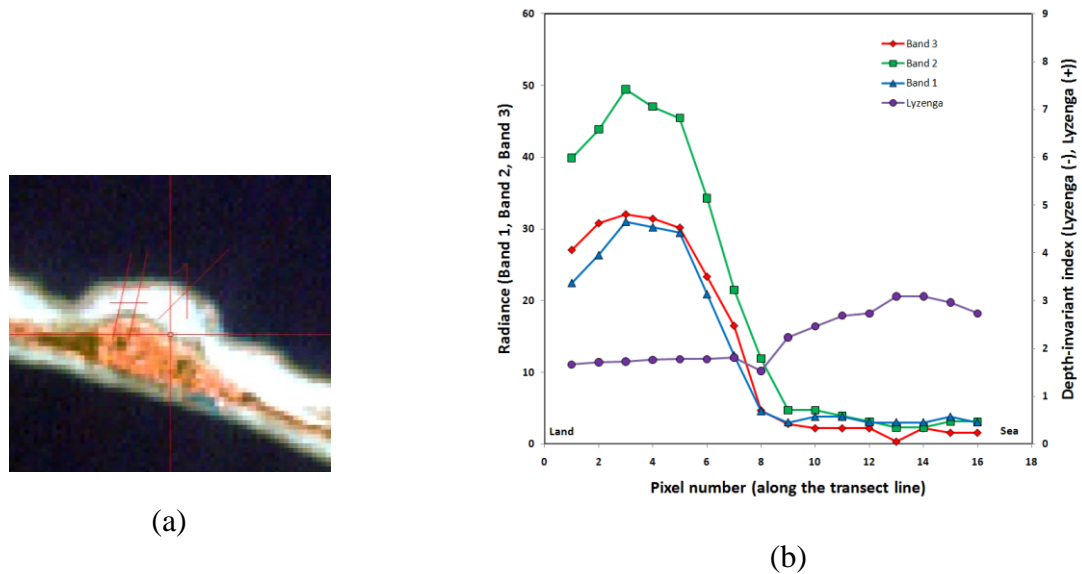


Figure 7. Transect line from landward to seaward (#1) (a), Graph of radiance value and depth-invariant index value within the transect line (#1) (b).

The same Landsat bands were used in this case study. Eight training samples site were selected (Figure 8) with total of 183 pixels. Figure 9 shows the graph between two Landsat bands and its attenuation coefficient (k_i/k_j). The result ratio k_i/k_j were 0.7512 (k_1/k_2), 0.2982 (k_1/k_3) and 0.4021 (k_2/k_3). The graphs in Figure 9 were based on sand type bottom substrate with different depth. All pixels spread around the linear line trend, with coefficient of determination (R^2) more than 0.98.

Figure 10 shows the result of water column correction. Transect line between point G to point H was made to observe the effect of different depth to bottom substrate radiance (Figure 10a). Figure 10b shows the radiance value before the water column correction. It clearly shows the effect of different depth to the radiance value of bottom substrate, where the deeper the water depth the lower the radiance value of the bottom substrate. This phenomena widely known as attenuation, which is the incoming radiance energy will be gradually reduce due to absorption by water and its constituents before it reach the object. Figure 10c shows the index value for the same pixel along the same transect line, which clearly shows that the effect of water depth has been eliminated. The graph shows most likely two types of

bottom substrates. The first type shown in the graph by pixel number 1-20 and pixel number 120-140, while the second type shown by pixel number 70-90. The first type most probably is sand, because the index values are higher than the second type. The second type could be coral reef or sea grass meadow, due to their low index value (UNESCO, 1999; Green *et al.*, 2000).

The three pairs of image after water column correction from different k_i/k_j ratio were used to make a false color composite (FCC) image. This FCC image is shown in Figure 11b. Figure 11a shows the FCC image of three different bands before water column correction. The figure 11b shows that the bottom substrate more detail compares to Figure 11a, because the water depth effect that exist in Figure 11a has been eliminated in Figure 11b. The blue color from ratio of band 1 and band 2 dominated the center part of the atoll, because the energy from spectrum of band 1 and band 2 can penetrate deeper to the water column. The ratio of band 2 and band 3 is helpful to identified chlorophyll pigment in the bottom substrate, because the peak of light absorption by chlorophyll pigment occurred in band 3 (~700 nm) (Kirk, 1994). The bright red color in Figure 11b (around upper left of the figure) could be dense seagrass

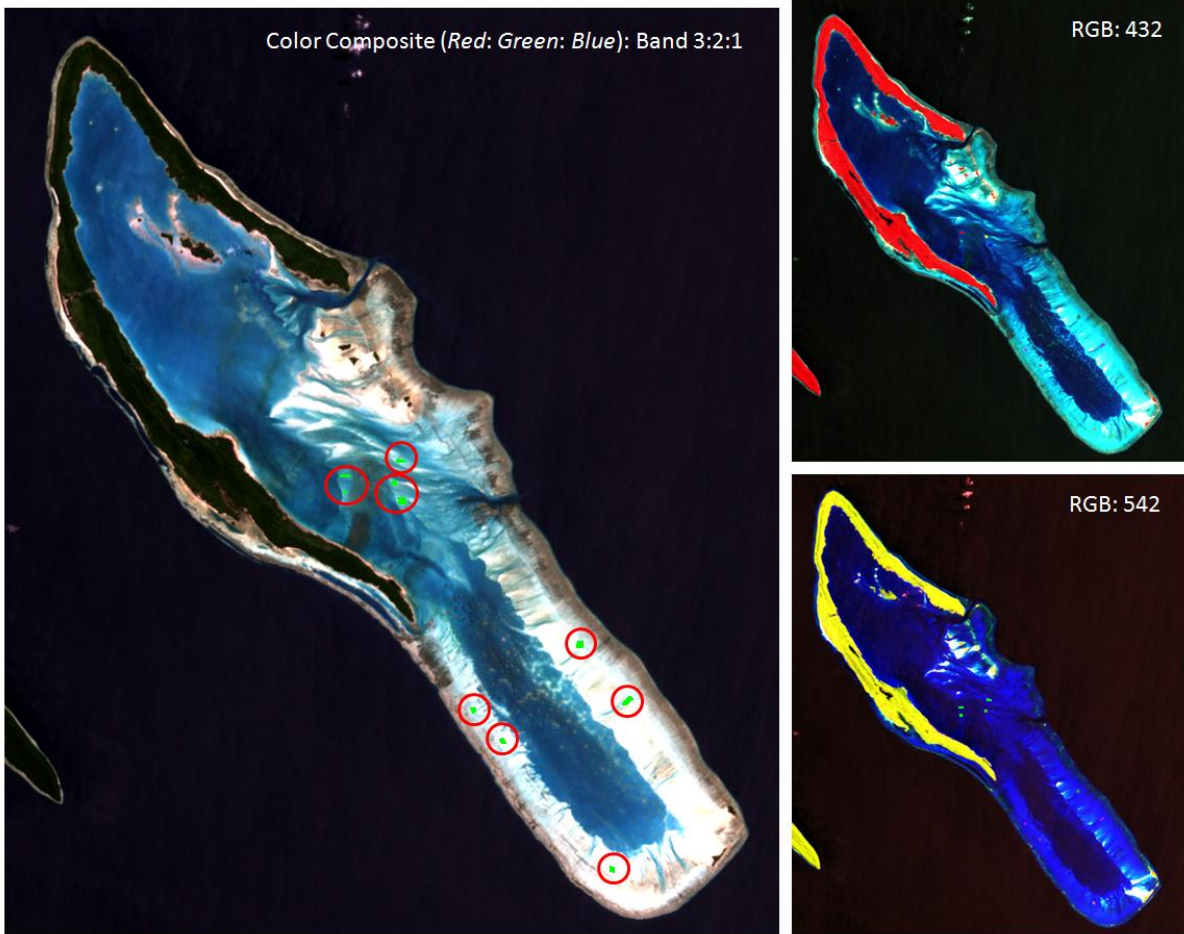


Figure 8. Three different color composite of Landsat ETM data (RGB 321, RGB 432 and RGB 542) of Maratua island and training sample site selection (circled).

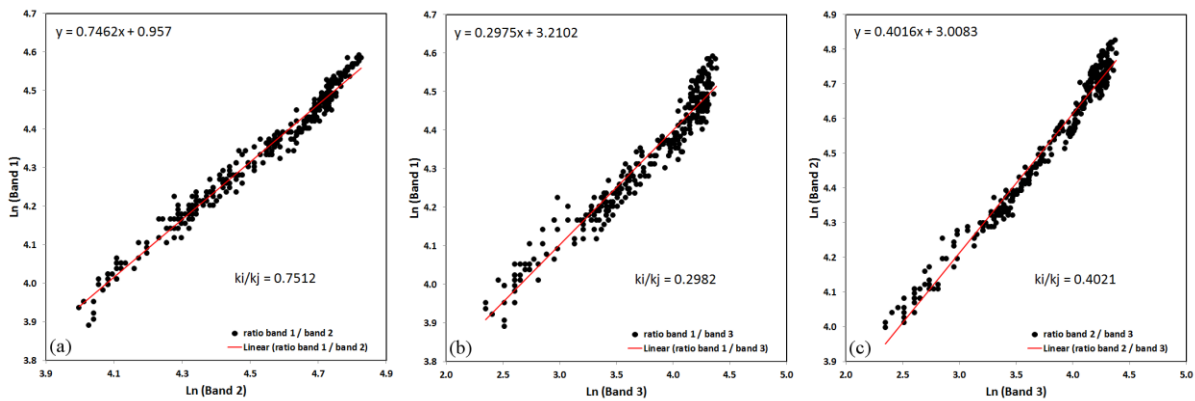


Figure 9. Graph of two pair bands in logarithmic scale and its coefficient attenuation for Maratua Island image using (a) ratio of band 1 and band 2, (b) ratio of band 1 and band 3, and (c) ratio of band 2 and band 3.

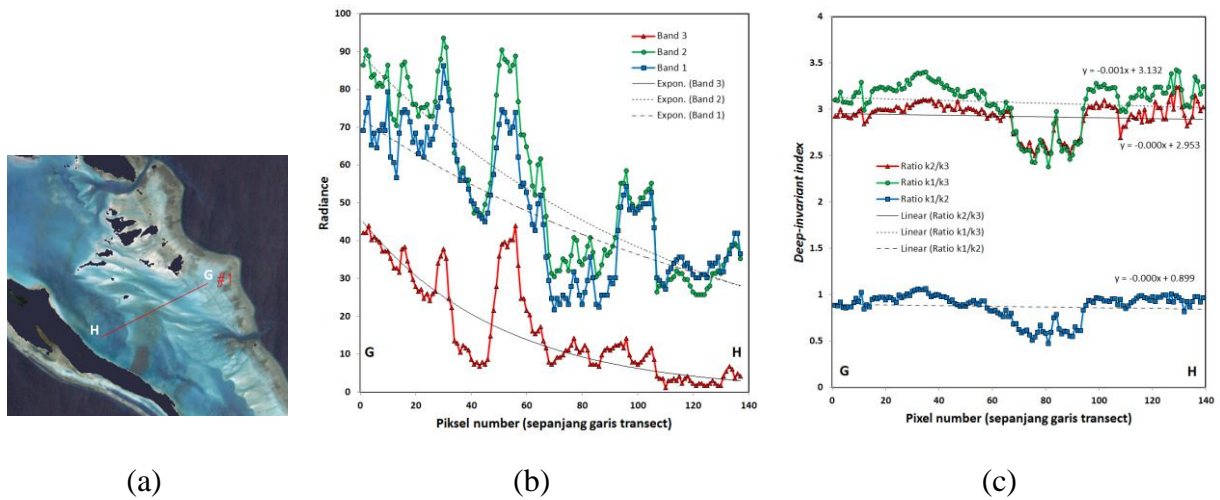


Figure 10. Transect line from point G to point H (a), radiance value of pixels number along the transect line from G to H (b), and depth-invariant index value along the transect line along the transect line from G to H (c).

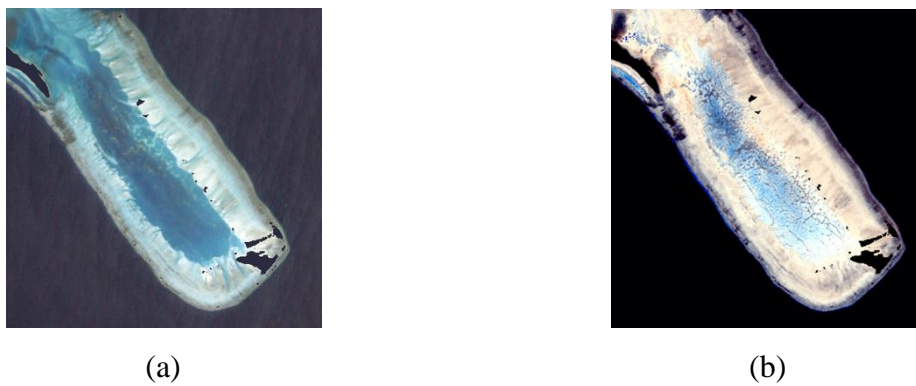


Figure 11. False color composite RGB (Red, Green, Blue) of band 3 (Red) band 2 (Green) and band 1 (Blue) (a), and water column corection image with ratio k_2/k_3 (Red), water column corection image with ratio k_1/k_3 (Green), and water column corection image with ratio k_1/k_2 (Blue) (b).

or macroalgae, while reddish color could be some patchy sea grass mixed with sand dominated bottom substrate.

3.3 Evaluation the effect of extent of the coral reef in training sample site selection

The 30 m Landsat spatial resolution and the extent of coral reef area are very influential in determining the training sample site location, as shown in the case of Tidung island. Bottom substrate identification at different depths was quite difficult in Tidung island, because the island size was relatively

small. Whereas in the case of Maratua island, it was easier to select training sample location site for bottom substrate with different depths. The problem of spatial resolution has been described by Mumby *et al.* (1997), which explained that the Landsat data was more influential in mapping coral reefs to the area more than 60 km (length and width of the coral reefs area).

The comparison between the attenuation ratio of Tidung island and Maratua island with the the ratios obtained from several literatures (Table 1). The attenuation ratio of the Maratua island was similar with the

attenuation ratios in the waters of the Bahamas (Armstrong, 1993), in the waters of the Turks and Caicos Islands (Green *et al.*, 2000), and in Red Sea, Egypt (Vanderstraete *et al.*, 2004). The results from case study of Tidung island showed higher value compare to that in Maratua island and from literature (Table 1). The result showed that for relatively small area of coral reef, one have to be cautious on finding uniform bottom reflectance on different depth using moderate spatial resolution image. The high

attenuation value found in Tidung island could be due to the same water depth of the sampled bottom reflectance and or water turbidity. All coral reefs areas except at Tidung island has clear water area, while in Tidung island (small coral reef area) has relatively turbid water. The radiance spectrum will increase due to the existing of turbidity and could increase the result of water column correction, hence the high value of ratio attenuation.

Table 1. Ratio of attenuation coefficients k_i/k_j from literature, Tidung island and Maratua island.

Location	Sensor and band	Ratio of attenuation coefficients	Literature
Bahamas	Landsat TM 1/2	0.74	Armstrong (1993)
	Landsat TM 1/3	0.36	Armstrong (1993)
	Landsat TM 2/3	0.49	Armstrong (1993)
Turks and Caicos island	Landsat TM 1/2	0.93	Green et al (2000)
Turks and Caicos island	Landsat TM 1/3	0.31	Green <i>et al.</i> (2000)
Turks and Caicos island	Landsat TM 2/3	0.36	Green <i>et al.</i> (2000)
Red Sea	Landsat ETM 1/2	0.75	Vanderstraete <i>et al.</i> (2004)
Red Sea	Landsat ETM 1/3	0.33	Vanderstraete <i>et al.</i> (2004)
Red Sea	Landsat ETM 2/3	0.52	Vanderstraete <i>et al.</i> (2004)
Tidung island	Landsat ETM 1/2	1.21	This research
Tidung island	Landsat ETM 1/3	1.22	This research
Tidung island	Landsat ETM 2/3	0.99	This research
Maratua island	Landsat ETM 1/2	0.75	This research
Maratua island	Landsat ETM 1/3	0.29	This research
Maratua island	Landsat ETM 2/3	0.40	This research

4 Conclusion

The water column correction of Landsat data was more effective applied in the large area of coral reefs ecosystem. In larger area of coral reef ecosystems, the possibility to find an uniform bottom substrate in different water depth on 30 meter Landsat spatial resolution was higher compare to the small area of coral reef. The results were confirmed with the similarity of the coefficient attenuation ratio from Maratua island with

those several places. On the other hand, the water depth in Tidung island which was relatively shallow, and the existence of mixed pixel between sand and patchy sea grass, could be the cause of high ratio of attenuation in Tidung island.

ACKNOWLEDGMENT

We would like to express our deep thanks to the reviewers for their useful comments and suggestions.

REFERENCES

- Adi, N.S., 2003, The changes of coral reefs condition by the application of combination on Lyzenga method and autocorrelation technique on Landsat TM and ETM satellite imagery: case study in the core zone of national sea park of Karimunjawa, Thesis, Fakultas Geografi UGM (in Indonesian) (unpublished).
- Andrefouet, S., F.E. Muller-Karger, E.J. Hochberg, C. Hu, and K.L. Carder, 2001, Change detection in shallow coral reef environments using Landsat 7 ETM+ data, *Remote Sensing of Environment*, 78:150-162.
- Armstrong, R.A., 1993, Remote sensing of submerged vegetation canopies for biomass estimation, *International Journal of Remote Sensing*, 14:621-627.
- Contreras-Silva, A.I., A.A. Lopez-Caloca, F.O. Tapia-Silva, and S. Cerdeira-Estrada, 2012, Satellite remote sensing of coral reef habitats mapping in shallow waters at Banco Chinchorro Reefs, Mexico: a classification approach.
- Eakin, C.M., C.J. Nim, R.E. Brainard, C. Aubrecht, C. Elvidge, D.K. Gledhill, F. Muller-Karger, P.J. Mumby, W.J. Skirving, A.E. Strong, M. Wang, S. Weeks, F. Wentz, and D. Ziskin, Monitoring coral reefs from space, *Oceanography*, 23(4):118-133.
- Green, E.P., P.J. Mumby, A.J. Edward, and C.D. Clark, 2000, Remote sensing handbook for tropical coastal management, UNESCO.
- Hamylton, S., 2011, An evaluation of waveband pairs for water column correction using band ratio methods for seabed mapping in the Seychelles, *International Journal of Remote Sensing*, 32(24):9,185-9,195.
- Hedley, J., C. Roelfsema, B. Koetz, and S. Phinn, 2012a, Capability of the Sentinel 2 mission for tropical coral reef mapping and coral bleaching detection, *Remote Sensing of Environment*, 120:145-155.
- Hedley, J., C.M. Roelfsema, S.R. Phinn, and P.J. Mumby, 2012b, Environmental and sensor limitations in optical remote sensing of coral reefs: implications for monitoring and sensor design, *Remote Sensing*, 4:271-302.
- Helmi, M., A. Hartoko, S. Herkiki, and S. Wouthuyzen, 2011, Spectral response analysis and spectral value extraction of coral reefs on multispectral digital imagery of ALOS-AVNIR satellite in Pari Islands, Seribu Islands, Jakarta, *Bulletin of Oceanography and Marine Science*, 1:120-136 (in Indonesian).
- Joyce, K.E., S.R. Phinn, C.M. Roelfsema, D.T. Neil, and W.C. Dennison, 2004, Combining Landsat ETM+ and reef check classifications for mapping coral reefs: a critical assessment from the southern Great Barrier Reef, Australia, *Coral Reefs*, 23:21-25.
- Kirk, J.T.O., 1994, Light and photosynthesis in aquatic ecosystems. New York: Cambridge Univ. Press.
- Kustiyo, N. Suwargana, Silvia, and J. S. Cahyono, 2006, Updating spatial information of entire Indonesian coastal natural resources, *Final Report LAPAN* (in Indonesian).
- Lyzenga, D.R., 1978, Passive remote sensing techniques for mapping water depth and bottom feature, *Applied Optics*, 17(3):379-383.
- Lyzenga, D.R., 1981, Remote sensing of bottom reflectance and water attenuation parameters in shallow water using aircraft and landsat data, *International Journal of Remote Sensing*, 2(1):71-82.
- Maritorea, S., 1996, Remote sensing of the water attenuation in coral reefs: a case study in French Polynesia, *International Journal of Remote Sensing*, 17(1):155-166.
- Mumby, P.J., E.P. Green, A.J. Edwards, and C.D. Clark, 1997, Coral reef habitat mapping: how much detail can remote sensing provide?, *Marine Biology*, 130:193-202.

- NASA, 2012, <http://landsathandbook.gsfc.nasa.gov/> [Retrieved 19 Februari, 2012].
- Purkis, S.J., and R. Pasterkamp, 2004, Integrating in situ reef-top reflectance spectra with Landsat TM imagery to aid shallow-tropical benthic habitat mapping, *Coral Reefs*, 23:5-20.
- Rauf, A., and M. Yusuf, 2004, Study of distribution and condition of coral reefs using remote sensing technology in Spermonde Islands, South Sulawesi, *Journal of Marine Sciences*, 9(2):74-81 (in Indonesian).
- Siregar, V.P., 2010, Mapping of shallow water substrate of Congkak and Lebar Reefs, Seribu Islands using Quick Bird satellite imagery, *E-Journal of Tropical Marine Science and Technology*, 2(1):19-30 (in Indonesian).
- Suciati, and I.W. Arthana, 2008, Study of coral reef distribution around Badung Strait using ALOS satellite data. *Ecotropic, Journal of Environmental Science*, 3(2):87-91.
- UNESCO, 1999, Applications of Satellite and Airborne Image Data to Coastal Management. Coastal region and small island papers 4. Paris: UNESCO.
- Vanderstraete, T., R. Goossens, and T.K. Ghabour, 2004, Coral reef habitat mapping in the Red Sea (Hurghada Egypt) based on remote sensing, *EARSel eProceedings*, 3(2):191-207.
- Wiryanawan, B., M. Khazali, and M. Knight, 2005, Toward marine conservation area of Berau, East Kalimantan: coastal resources status and the development process of marine conservation area, http://www.rareplanet.org/sites/rareplanet.org/files/Tugas_COMM_5311_ringkasan_eksekutif.pdf, [Retrieved February 13, 2012 (in Indonesian)].
- Yamano, H., and M. Tamura, 2004, Detection limits of coral reef bleaching by satellite remote sensing: simulation and data analysis, *Remote Sensing of Environment*, 90:86-103.